Electronic Supplementary Material (ESI) for Dalton Transactions

Iron(II) and Cobalt(II) Complexes of Tris-Azinyl Analogues of 2,2':6',2''-Terpyridine

Laurence J. Kershaw Cook,[a] Floriana Tuna,[b] and Malcolm A. Halcrow[a,]*

[a]School of Chemistry, University of Leeds, Woodhouse Lane, Leeds LS2 9JT, U.K..
[b]School of Chemistry, University of Manchester, Oxford Road, Manchester M13 9PL, UK
Email: M.A.Halcrow@leeds.ac.uk

Supporting Information

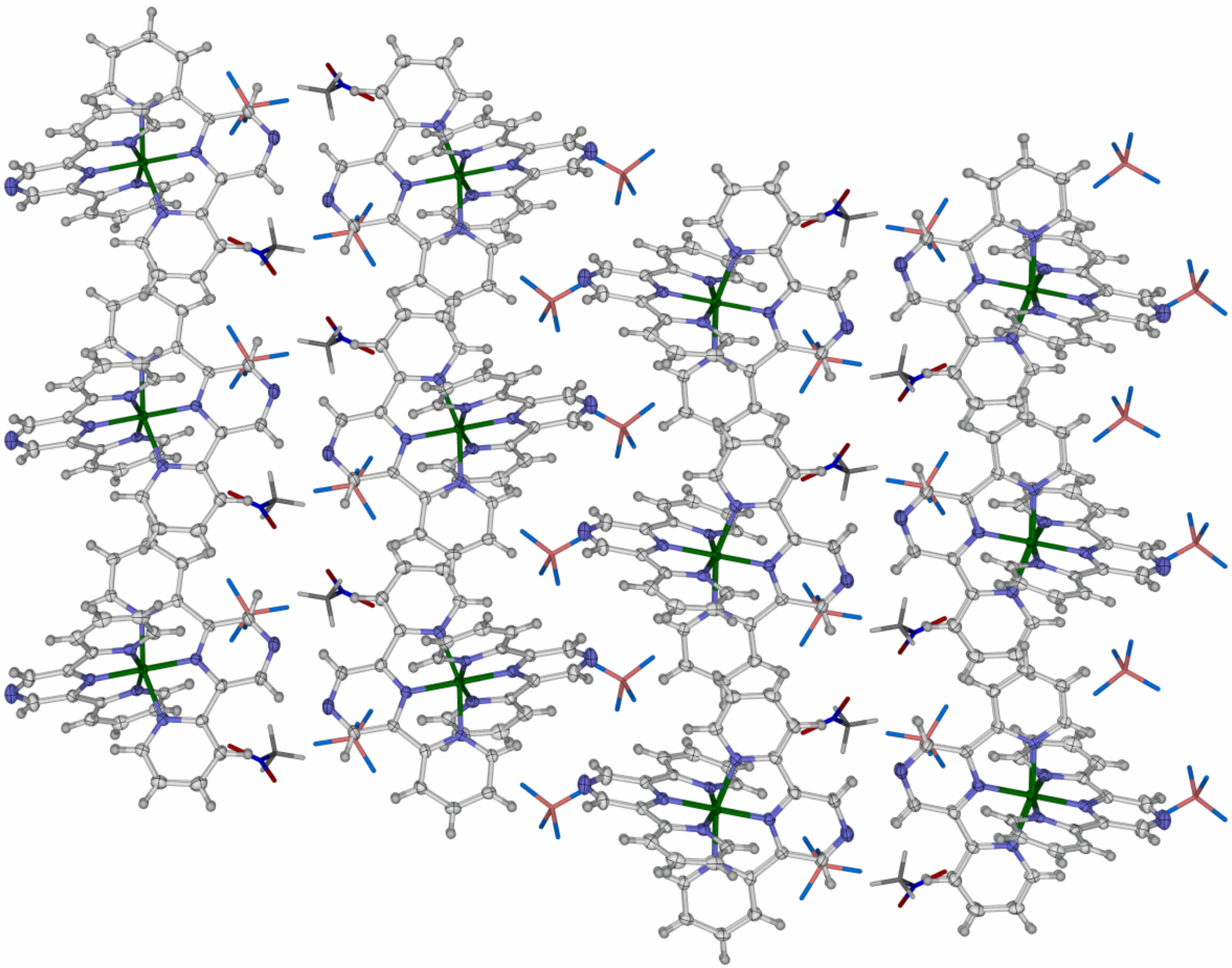

Figure S1. Partial packing diagram for **1a**·$MeNO_2$. The view is perpendicular to the (100) crystal plane, and only one orientation of the disordered anion and solvent residues is shown. Displacement ellipsoids are at the 50 % probability level except for the BF_4^- ions and nirtomethane molecules, which have been de-emphasised for clarity. Colour code: C, white; H, grey; B, pink; F, cyan; Fe, green; N, blue; O, red.

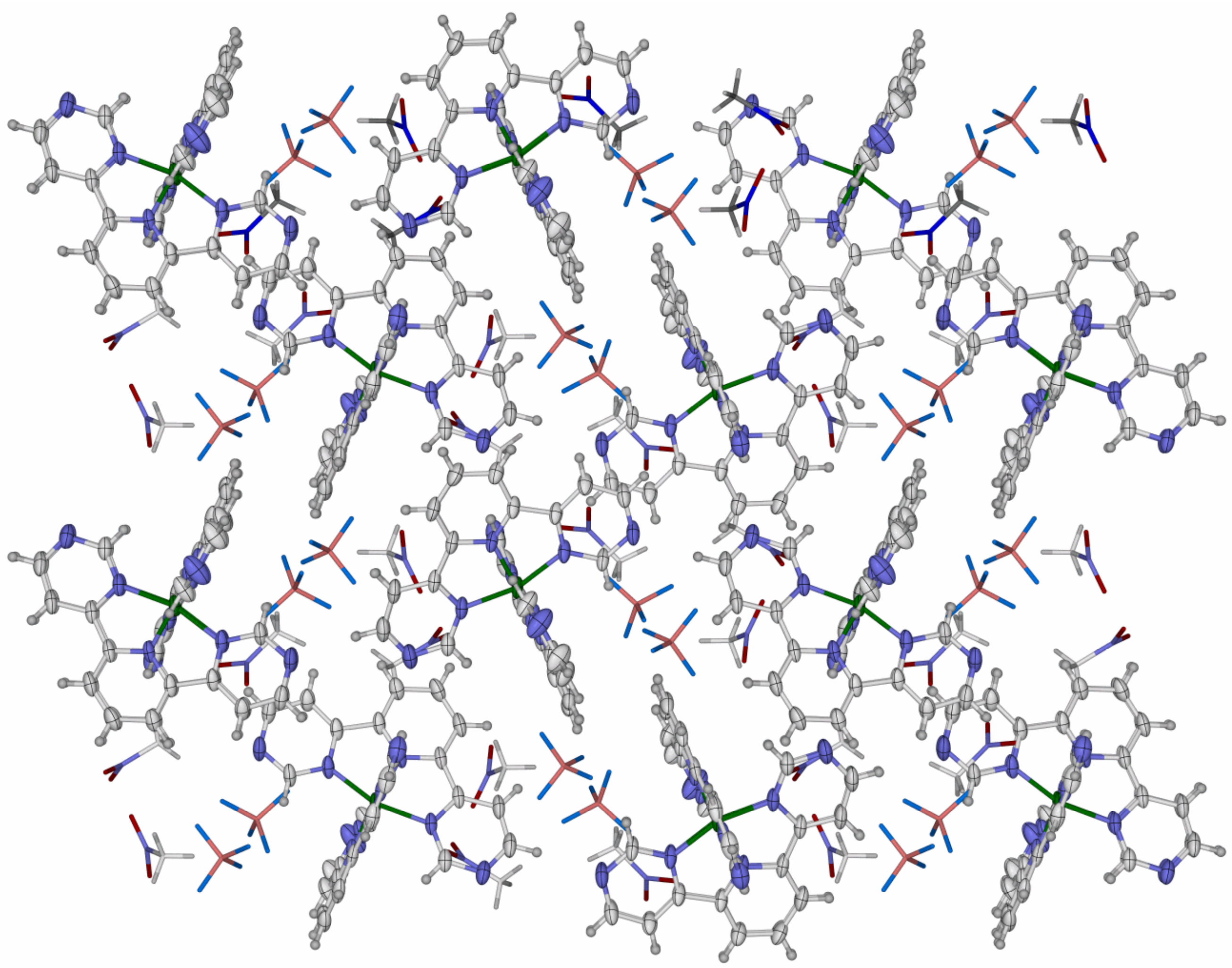

Figure S2. Partial packing diagram for **1d**·3MeNO$_2$. The view is perpendicular to the (100) crystal plane, and only one orientation of the disordered anion and solvent residues is shown. Displacement ellipsoids are at the 50 % probability level except for the BF$_4^-$ ions and nirtomethane molecules, which have been de-emphasised for clarity. Colour code: C, white; H, grey; B, pink; F, cyan; Fe, green; N, blue; O, red.

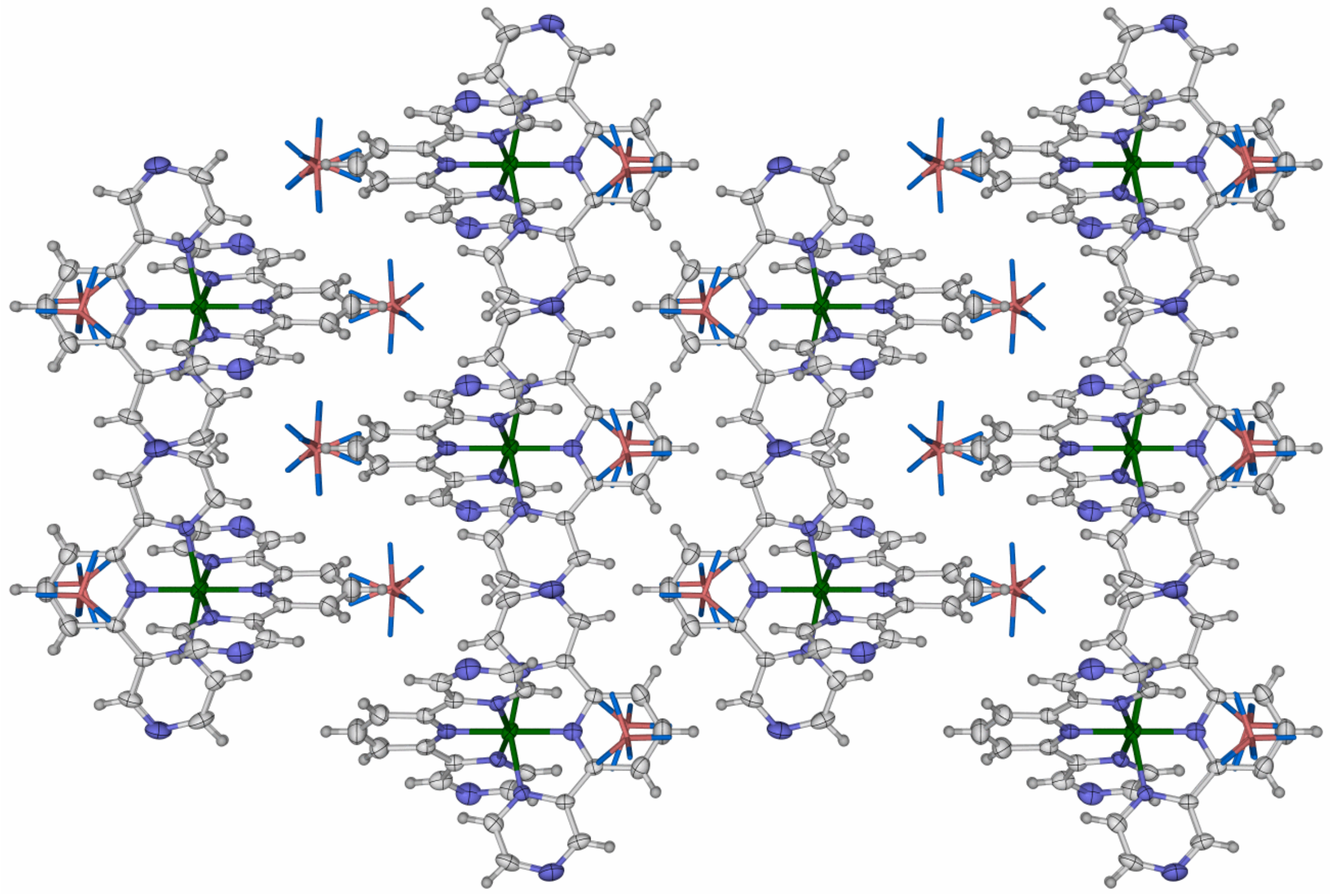

Figure S3. Partial packing diagram for **2b**. The view is perpendicular to the (100) crystal plane, and only one of the two BF_4^- environments in each anion site is shown. Displacement ellipsoids are at the 50 % probability level except for the BF_4^- ions which have been de-emphasised for clarity. Colour code: C, white; H, grey; B, pink; Co, green; F, cyan; N, blue.

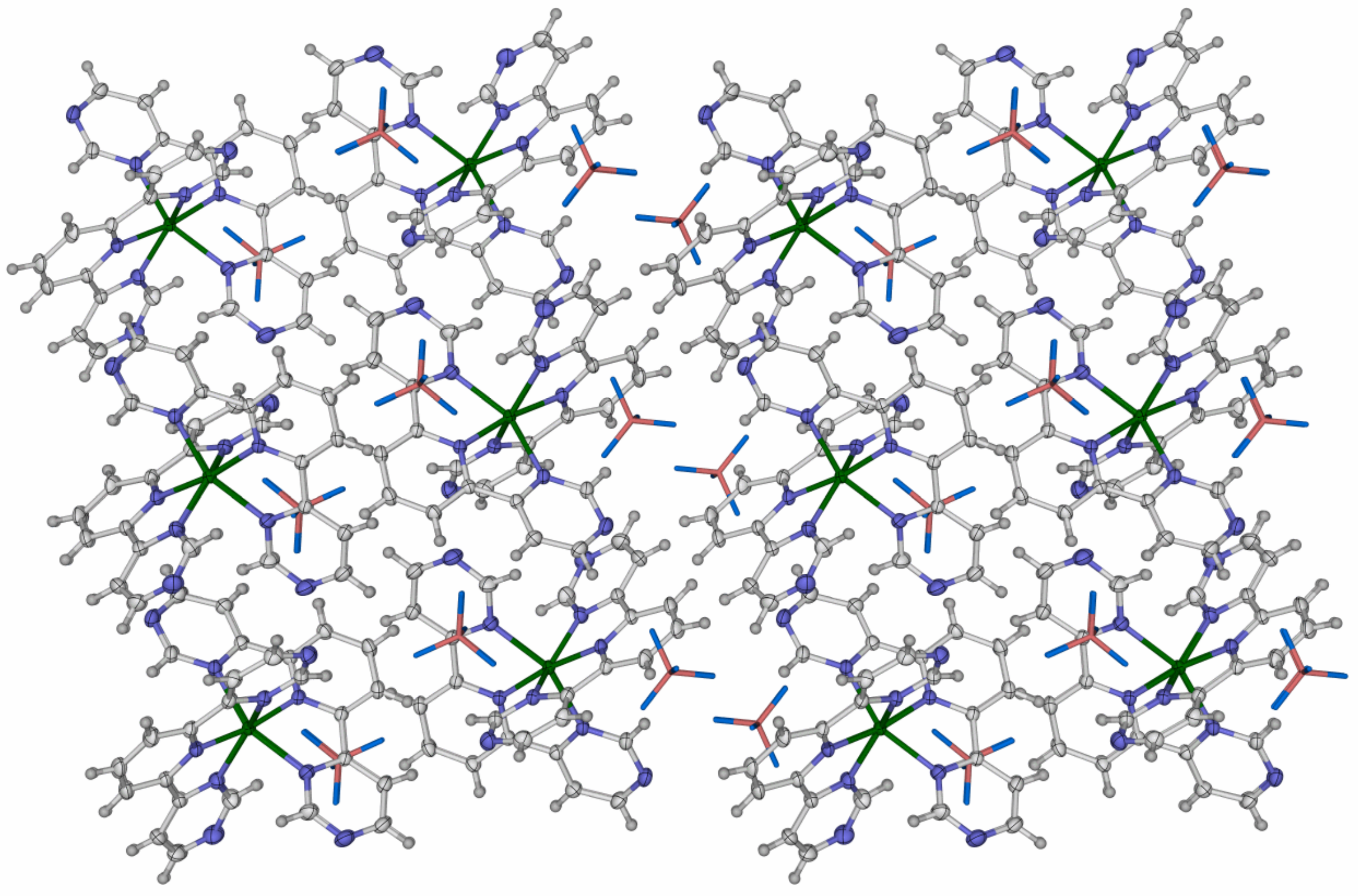

Figure S4. Partial packing diagram for **2d**. The view is perpendicular to the (010) crystal plane, and only one orientation of the disordered anion is shown. Displacement ellipsoids are at the 50 % probability level except for the BF_4^- ions which have been de-emphasised for clarity. Colour code: C, white; H, grey; B, pink; Co, green; F, cyan; N, blue.

Table S1. Metric parameters for intermolecular π-π interactions in crystal structures in this work (Å, °). Symmetry codes: (i) *x*, *y*, *z*; (ii) *x*, –1+*y*, *z*; (iii) –*x*, 1–*y*, *z*.

	Dihedral angle	Interplanar spacing	Horizontal offset
1a·$MeNO_2$			
[C(8)-C(13)]...[C(14^{i})-C(19^{i})]	7.1(2)	3.345(15)	1.80
[C(26)-C(31)]...[C(32^{ii})-C(37^{ii})]	1.95(18)	3.452(16)	2.07
2b			
[C(6)-C(11)]…[C(6^{iii})-C(11^{iii})]	1.01(14)	3.567(14)	1.18

There are no intermolecular π-π interactions in the structures of **1d**·$3MeNO_2$ and **2d**.

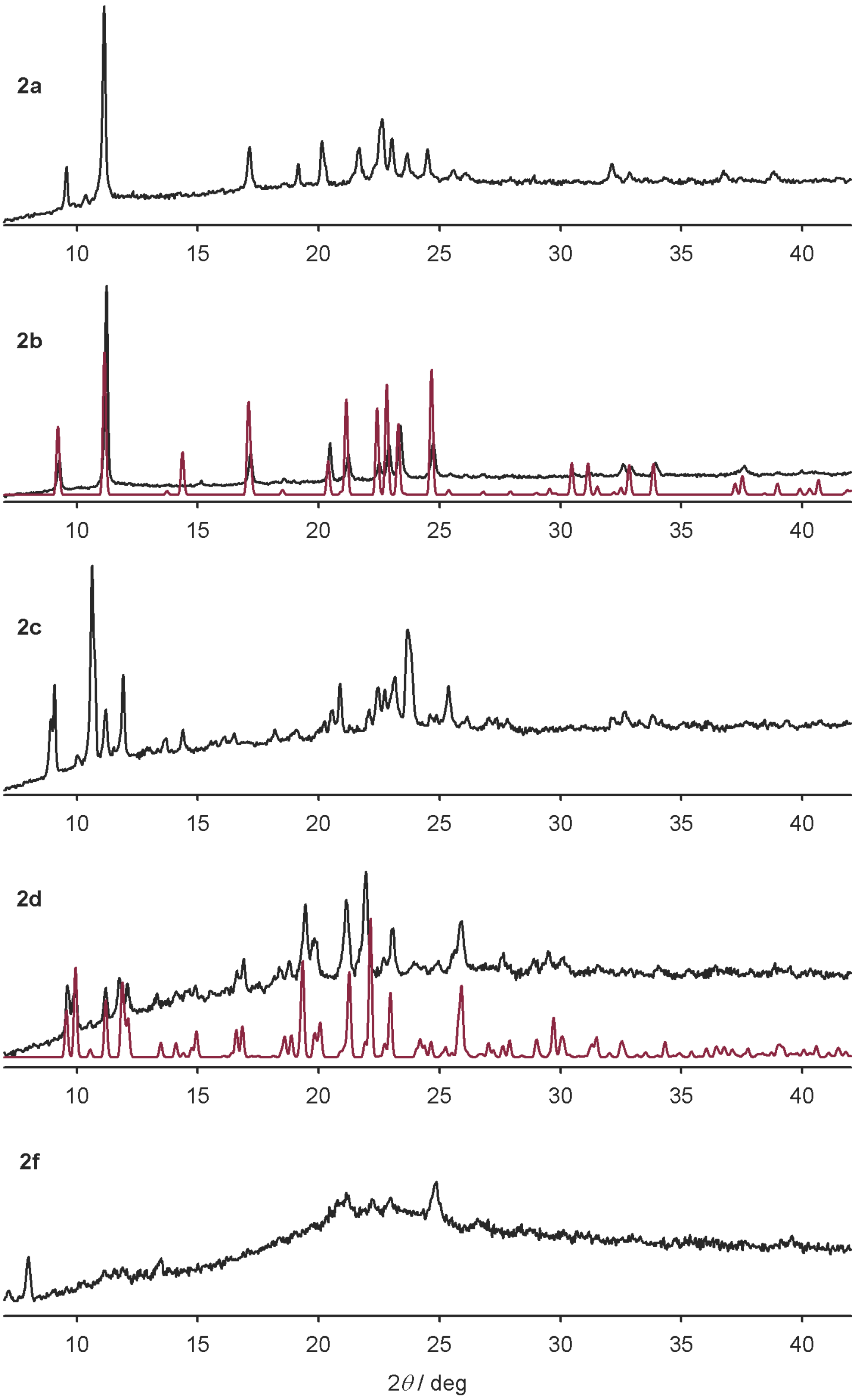

Figure S5. Selected *X*-ray powder diffraction data from cobalt complexes in this work. Simulations based on the single crystal *X*-ray structures of **2b** and **2d** are shown in red.

Table S2. *X*-band powder EPR parameters for the cobalt compounds in this work (Figs. S1 and S2). The quoted g and A values are the results of simulations, and hyperfine couplings are to ^{59}Co ($I = {}^{7}/_{2}$). iso = isotropic; br = broad; w = weak.

	120±5 K	180 K	290 K
$[Co(terpy)_2][BF_4]_2$[4]	axial; $g_{\parallel} = 2.22$ $g_{\perp} = 2.12$	iso; $g = 2.12$	–[a]
$[Co(terpyOH)_2][BF_4]_2$	iso; $g = 2.11$	iso; $g = 2.12$	–[a]
$[Co(L^1)_2][BF_4]_2$ (**2a**)	axial; $g_{\parallel} = 2.22$[b] $g_{\perp} = 2.12$	iso; $g = 2.12$	–[a]
$[Co(L^2)_2][BF_4]_2$ (**2b**)	iso; $g = 2.11$	iso; $g = 2.12$	br w iso; $g = 2.14$
$[Co(L^3)_2][BF_4]_2$ (**2c**)	iso; $g = 2.11$	iso; $g = 2.11$[b]	iso; $g = 2.15$
$[Co(L^4)_2][BF_4]_2$ (**2d**)	axial; $g_{\parallel} = 2.23$, $A_{\parallel} = 98$ G $g_{\perp} = 2.13$	axial; $g_{\parallel} = 2.20$, $A_{\parallel} = 88$ G $g_{\perp} = 2.13$	w axial; $g_{\parallel} = 2.18$, $A_{\parallel} = 87$ G $g_{\perp} = 2.13$
$[Co(L^5)_2][BF_4]_2$ (**2e**)	iso; $g = 2.12$[b]	iso; $g = 2.12$[b]	w iso; $g = 2.11$[b]
$[Co(L^5)_2][BF_4]_2$ (**2f**)	iso; $g = 2.12$	iso; $g = 2.12$	br w iso; $g = 2.14$
$[Co(L^6)_2][BF_4]_2$ (**2g**)	axial; $g_{\parallel} = 2.23$, $A_{\parallel} = 100$ G $g_{\perp} = 2.12$	br iso; $g = 2.12$[b]	–[a]

[a] EPR-silent. [b] Some evidence for hyperfine coupling is apparent in the parallel region of this spectrum, but the lines were too broad to simulate accurately.

The best resolved low-temprature spectra are shown by **2d** and **2g**, which also have the smallest low-spin populations at 120 K (Table S1). Thus, those two samples have the most magnetically dilute $S = {}^{1}/_{2}$ cobalt centres, at a temperature where dipolar relaxation by the remainder $S = {}^{3}/_{2}$ cobalt sites is weak.

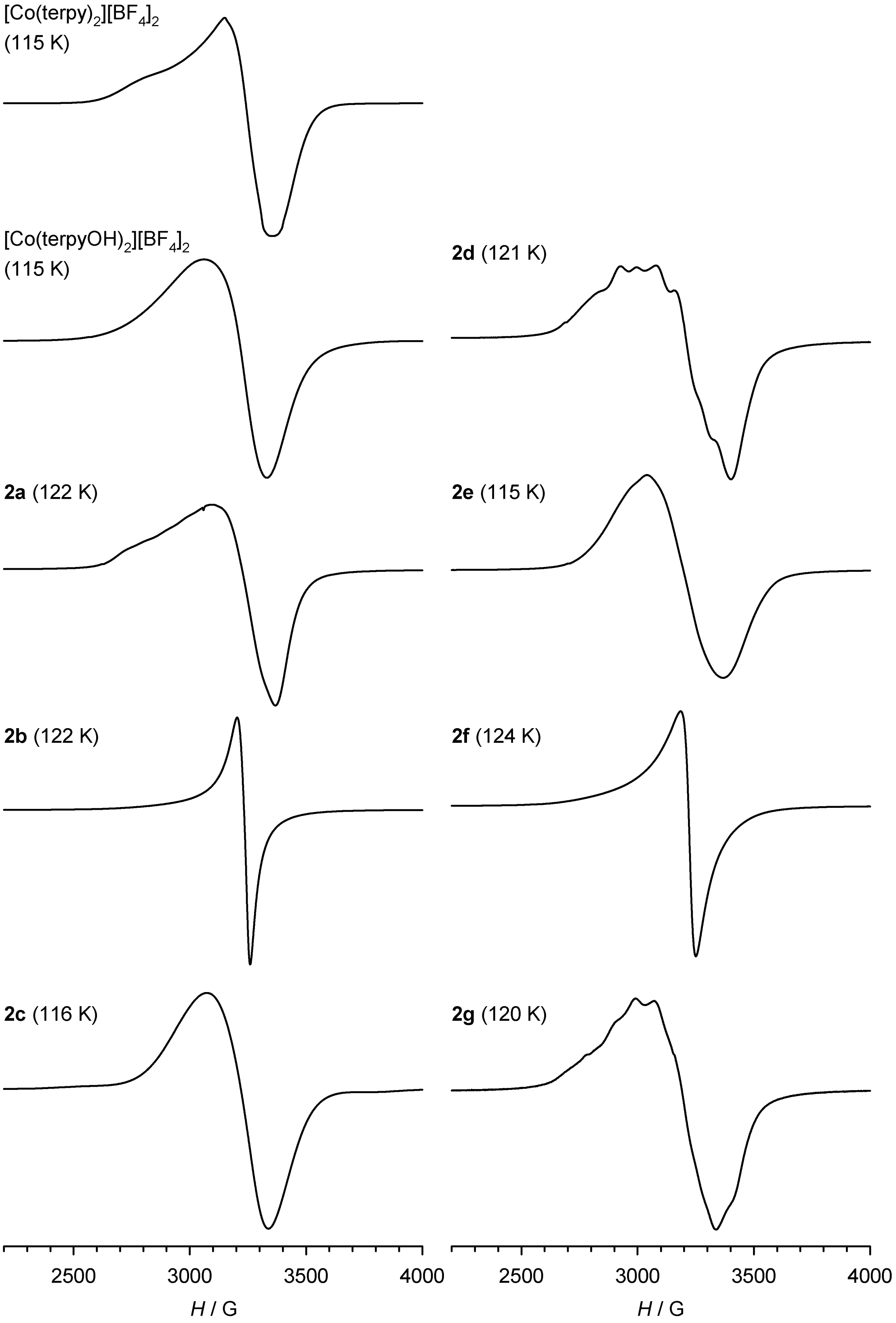

Figure S6. Powder *X*-band EPR spectra of the cobalt(II) complexes in this work, at around 120 K. The spectrum of [Co(terpy)$_2$][BF$_4$]$_2$ is taken from ref. [4].

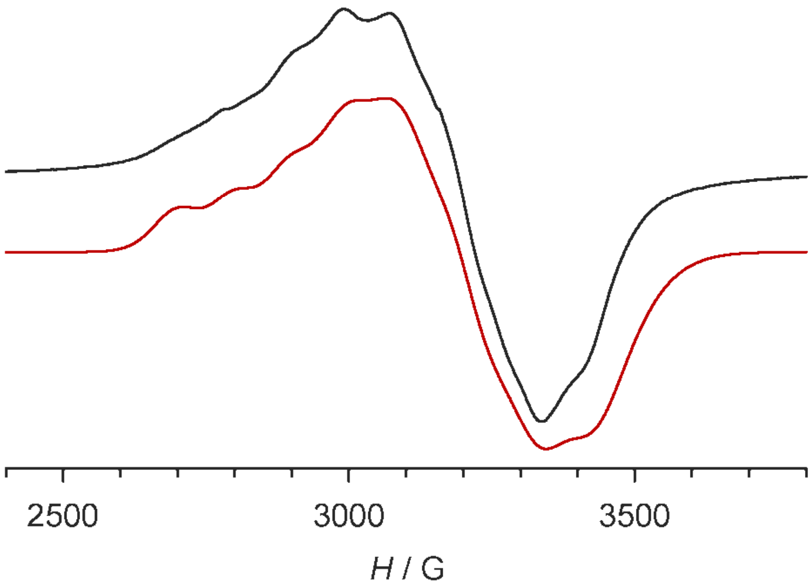

Figure S7. Experimental (black) and simulated (red) *X*-band powder EPR spectrum of **2g** at 120 K. Simulation parameters: $g_{||}$ = 2.23, $g_{\perp}$ = 2.13, $A_{||}\{^{59}\mathrm{Co}\}$ = 100 G.

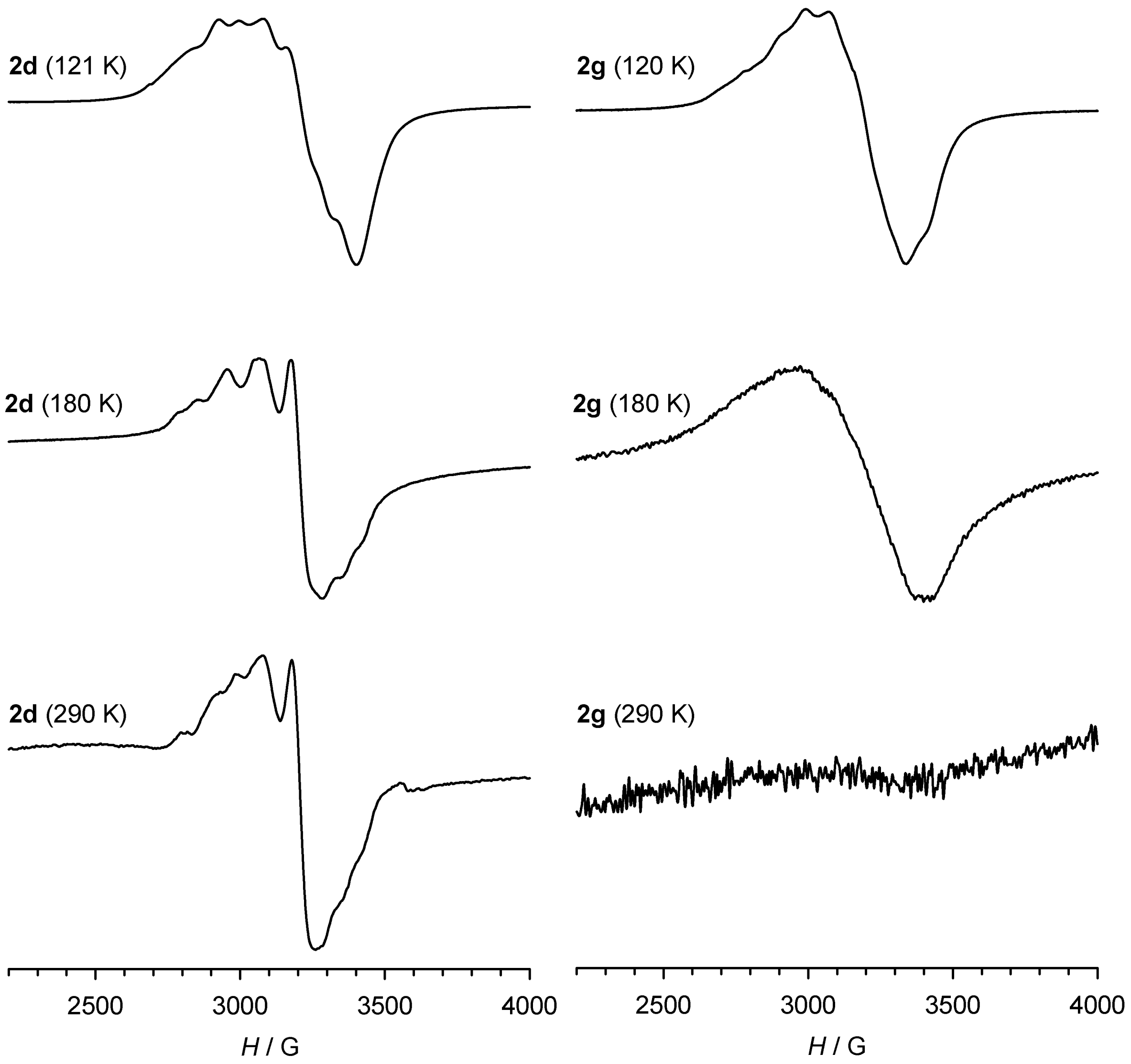

Figure S8. Variable temperature powder *X*-band EPR data for **2d** and **2g**.

The narrow linewidth and high resolution of the spectrum of **2d** at 290 K contrasts with most of the other compounds in this work. A similar lack of line-broadening is also shown by **2c** at higher temperatures, although its spectrum is not so well resolved (Fig. S1). Solid **2c** and **2d** are predominantly low-spin, and high-spin, respectively at room temperature (Table S1, and Fig. 3 of the main paper).

The behaviour of **2g** at higher temperatures is typical of the other seven complexes studied.

Table S3 UV/vis data for the complexes in this work (MeCN, 298 K). Spectra for **1e** and **2e** were not measured, because of the difficulty in obtaining pure samples of those compounds. The data for $[M(terpy)_2][BF_4]_2$ (M^{2+} = Fe^{2+} and Co^{2+}) closely resemble the spectra reported for salts of those compounds in other solvents.[5,6]

	λ_{max}, nm (ε_{max}, 10^3 dm^3 mol^{-1} cm^{-1})
$[Fe(terpy)_2][BF_4]_2$	220 (sh), 273 (41.6), 280 (37.5), 319 (51.1), 504 (sh), 552 (11.1), 590 (sh)
$[Fe(terpyOH)_2][BF_4]_2$	243 (54.5), 272 (52.0), 281 (sh), 315 (45.0), 362 (5.1), 515 (sh), 553 (11.6)
1a	249 (sh), 278 (28.8), 328 (31.3), 345 (sh), 552 (7.9), 590 (sh)
1b	230 (36.4), 246 (sh), 285 (34.9), 330 (18.2), 350 (sh), 552 (3.1), 590 (sh)
1c	221 (36.5), 227 (sh), 243 (30.9), 282 (47.1), 339 (34.0), 360 (23.5), 462 (1.8), 545 (7.9), 580 (sh)
1d	220 (34.8), 263 (sh), 272 (26.1), 278 (sh), 315 (32.9), 319 (sh), 574 (5.7), 610 (sh)
1f	218 (21.6), 238 (24.9), 245 (sh), 283 (28.3), 323 (sh), 355 (sh), 483 (sh), 586 (2.7), 655 (sh)
1g	252 (54.6), 292 (sh), 305 (10.8), 397 (4.8), 545 (6.1)
$[Co(terpy)_2][BF_4]_2$	225 (sh), 273 (30.2), 280 (31.1), 317 (33.8), 506 (1.0), 551 (sh)
$[Co(terpyOH)_2][BF_4]_2$	228 (58.4), 275 (34.8), 303 (sh), 379 (7.2), 454 (0.7)
2a	280 (24.2), 337 (21.2), 348 (sh), 509 (1.1)
2b	288 (52.7), 332 (31.8), 511 (1.1)
2c	225 (33.5), 285 (41.4), 346 (19.6), 474 (sh), 510 (0.8), 558 (sh)
2d	263 (sh), 280 (sh), 315 (44.6), 521 (0.4)
2f	232 (27.8), 285 (18.0), 312 (sh), 386 (3.8), 499 (1.0)
2g	232 (40.6), 251 (52.7), 379 (4.7), 480 (0.8)

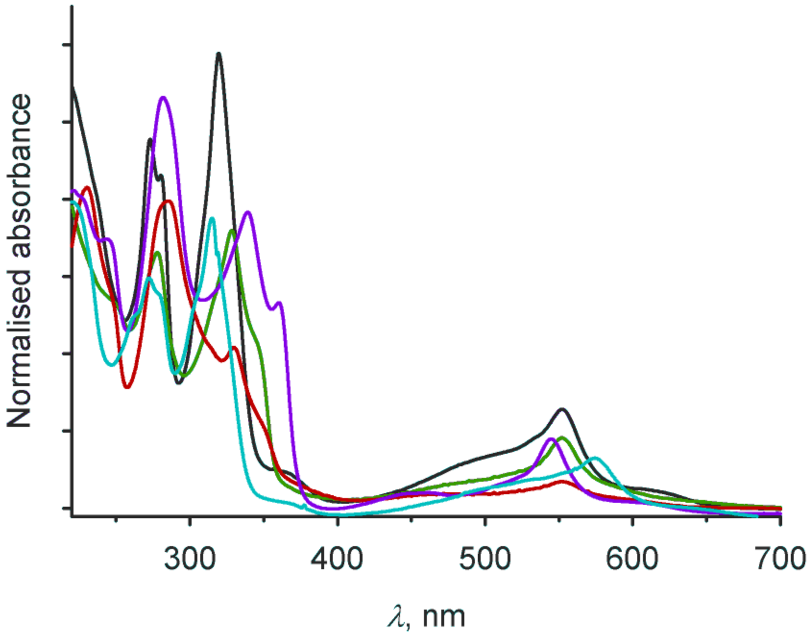

Figure S9. UV/vis spectra (MeCN, 298 K) of $[Fe(terpy)_2][BF_4]_2$ (black), **1a** (green), **1b** (red), **1c** (purple) and **1d** (cyan). These data are tabulated in the main paper.

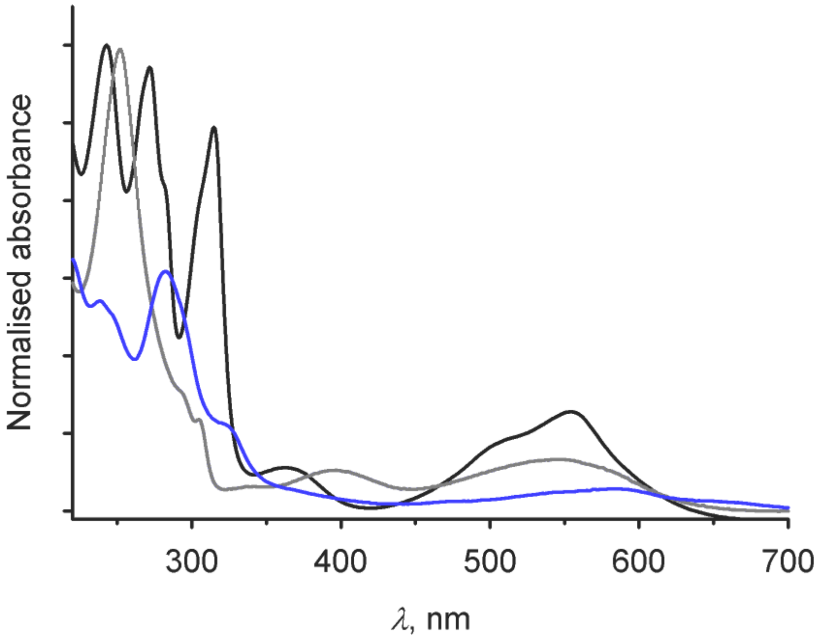

Figure S10. UV/vis spectra (MeCN, 298 K) of $[Fe(terpyOH)_2][BF_4]_2$ (black), **1f** (blue) and **1g** (grey). These data are tabulated in the main paper.

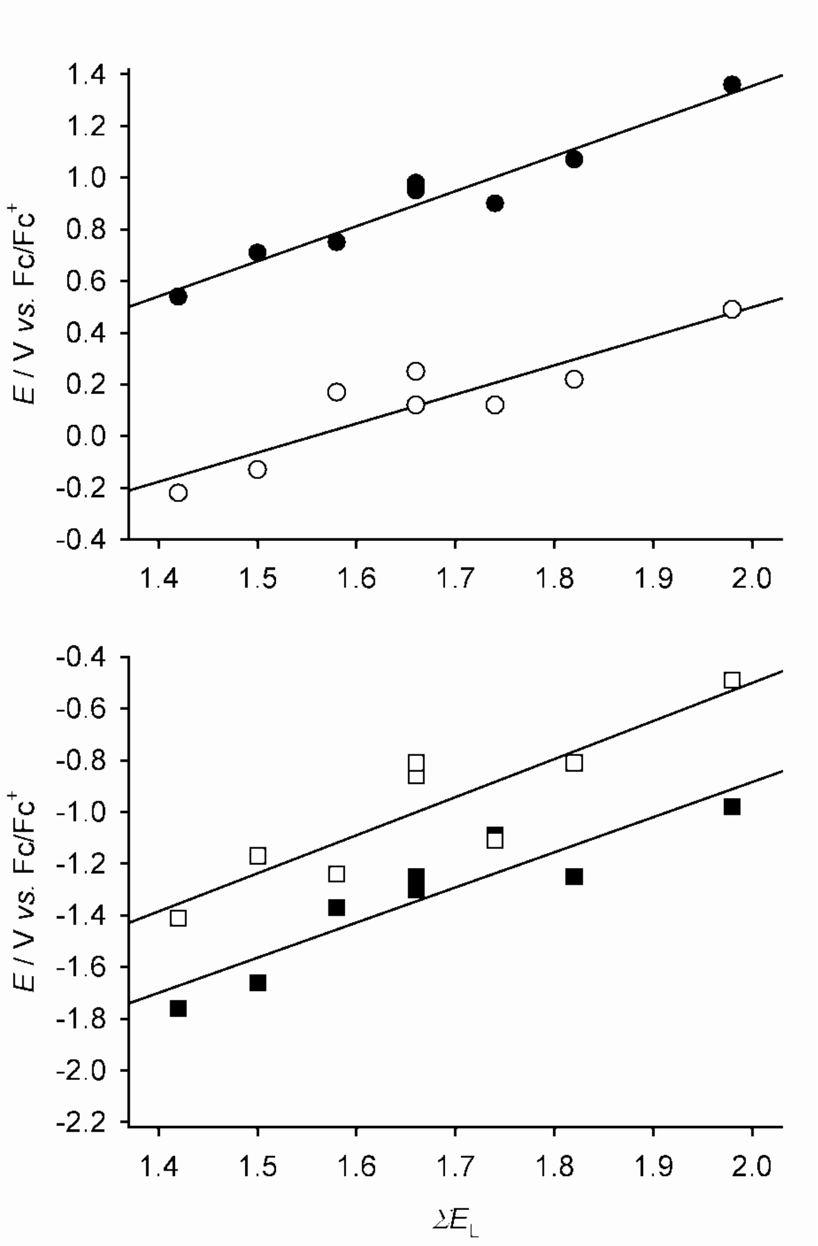

Figure S11. Correlations between $E_{½}$ and ΣE_L[7] for the oxidation (top) and first reduction (bottom) processes shown by the complexes: (●) iron oxidation; (○) cobalt oxidation; (■) iron reduction; (□) cobalt reduction. Ep_a or Ep_c peak potentials are plotted for irreversible processes, but this has only a small effect on the scatter in the graphs. These data are listed in Table 3 of the main article.

The E_L value for 4-hydroxypyridine employed in this analysis (0.21) is an estimated one, based on the published value of 4-(dimethylamino)pyridine (E_L = –0.19[8]) and the σ_p Hammett parameters for dimethylamino and hydroxy substituents, which are known to correlate with $E_{½}$ in $[M(terpy)_2]^{2+}$ derivatives (M^{2+} = Fe^{2+}, Co^{2+} and Ru^{2+}).[9] The complexes **1e** and **2e** are omitted from these graphs, because no E_L value for 1,2,4-triazine is available.

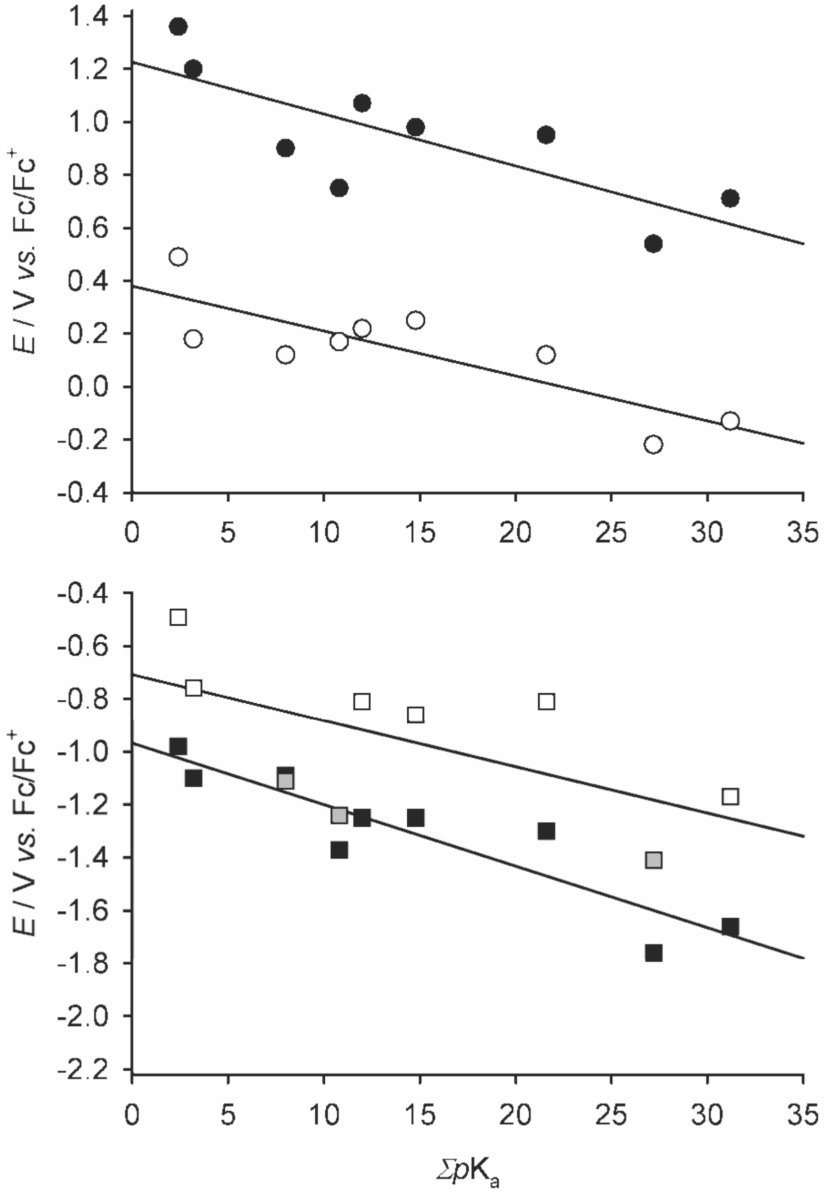

Figure S12. Correlations between $E_{½}$ and ΣpK_a for the oxidation (top) and first reduction (bottom) processes shown by the complexes: (●) iron oxidation; (○) cobalt oxidation; (■) iron reduction; (□ and ▨) cobalt reduction. Ep_a or Ep_c peak potentials are plotted for irreversible processes, but this has only a small effect on the scatter in the graphs. These data are listed in Table 3 of the main article.

The graphs are plotted to the same vertical scale as in Fig. S6, to aid comparison.

There is more scatter on the cobalt reduction plot than for the other processes in the Figure. The grey data points are the cobalt complexes of the hydroxylated ligands terpyOH, L^6 and L^7 which all show lower than expected E values compared to the other complexes in that series. That tentatively supports the suggestion in the main article that, among the cobalt reductions, the white data points are metal-based reductions while the grey data points may be ligand-based.

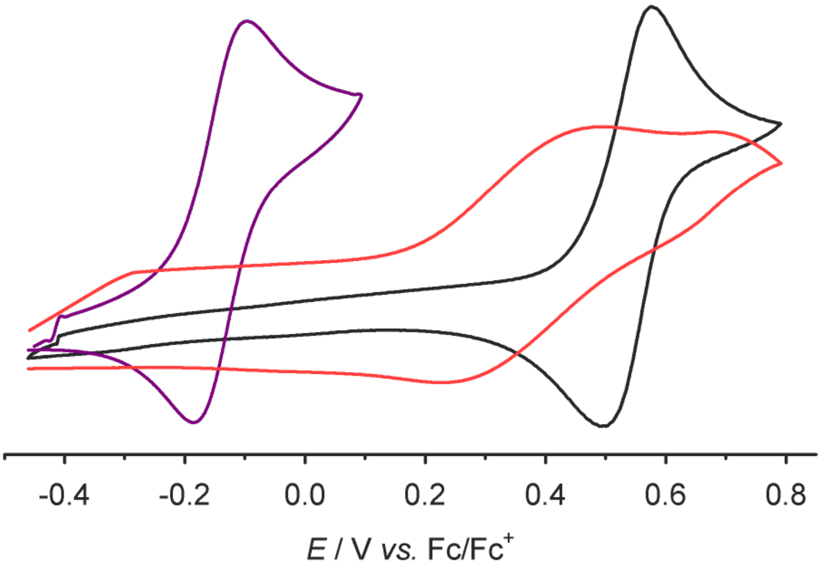

Figure S13. The Fe(III)/(II) couple in the cyclic voltammograms of the same solution of [Fe(terpyOH)$_2$][BF$_4$]$_2$ in the presence of 0 (black), 1 (red) and 2 (purple) equiv NBu$_4$OH (MeCN/0.1 M NBu$_4$BF$_4$, 298 K). These data are listed in Table 4 of the main article.

References

[1] G. Agustí, C. Bartual, V. Martínez, F. J. Muñoz-Lara, A. B. Gaspar, M. C. Muñoz and J. A. Real, *New J. Chem.*, 2009, **33**, 1262.

[2] C. J. O'Connor, *Prog. Inorg. Chem.*, 1982, **29**, 203.

[3] R. Boča, *Coord. Chem. Rev*., 2004, **248**, 757.

[4] C. A. Kilner and M. A. Halcrow, *Dalton Trans.*, 2010, **39**, 9008.

[5] P. S. Braterman, J.-I. Song and R. D. Peacock, *Inorg. Chem.*, 1992, **31**, 555;
T. G. Spence, B. T. Trotter and L. A. Posey, *J. Phys. Chem. A*, 1998, **102**, 7779.

[6] S. Kremer, W. Henke and D. Reinen, *Inorg. Chem.*, 1982, **21**, 3013.

[7] A. B. P. Lever, *Inorg. Chem.*, 1990, **29**, 1271.

[8] A. J. L. Pombeiro, *J. Organomet. Chem.*, 2005, **690**, 6021.

[9] M. Maestri, N. Armaroli, V. Balzani, E. C. Constable and A. M. W. Cargill Thompson, *Inorg. Chem.*, 1995, **34**, 2159;
J. Chambers, B. Eaves, D. Parker, R. Claxton, P. S. Ray and S. J. Slattery, *Inorg. Chim. Acta*, 2006, **359**, 2400.